

Investigation on temperature dependence of recent high-efficiency silicon solar modules

Chenhai Nan, Yuanpang Hao, Xin Huang, He Wang, Hong Yang*

MOE Key Laboratory for Nonequilibrium Synthesis and Modulation of Condensed Matter, School of Physics, Xi'an Jiaotong University, Xi'an, 710049, People's Republic of China



ARTICLE INFO

Keywords:

Temperature dependence
Solar modules
PERC
SHJ
TOPCon

ABSTRACT

The temperature dependence of photovoltaic modules varies with temperature and irradiance. For recent high-efficiency solar modules such as silicon heterojunction (SHJ) solar modules and tunneling oxide passivated contact (TOPCon) solar modules, it is not clear how their temperature dependence changes with temperature and irradiance. In this study, the temperature dependence of SHJ and TOPCon solar modules was studied by measuring I-V curves with the irradiance ranging from 200 to 1000 W/m² and temperature ranging from 25 to 75 °C. The passivated emitter and rear cell (PERC) solar modules were measured as a reference. The results indicate that the temperature dependence of short-circuit current (I_{sc}) for the three modules is almost invariable with temperature and irradiance. The temperature dependence of open-circuit voltage (V_{oc}) and maximum power (P_m) decreasees with the increasing module temperature, and increasees with the increasing irradiance. It can be observed that the absolute magnitude of $(\partial P_m / \partial T)/P_m$ for SHJ is the smallest, which is more obvious at high irradiance. An interesting finding is that the temperature dependence of fill factor (FF) for SHJ solar module increases with increasing irradiance, which is opposite to PERC and TOPCon solar modules. This phenomenon is related to the temperature dependence of series resistance. In addition, the temperature dependence is not linear at low temperature and irradiance. The obtained results in this paper can provide useful insight into predicting performance ratio of PERC, SHJ and TOPCon solar modules.

1. Introduction

The operating temperature of solar modules is usually higher than that of standard test conditions (STC: 1 kW/m² irradiance, 25 °C module temperature and AM 1.5 global spectrum), which strongly affects its output in the field. Therefore, studying on the temperature dependence of solar modules is very important to evaluate the actual output of solar modules. The structure of solar modules affects the temperature dependence of solar modules [1]. It is necessary to study the temperature dependence of recent high-efficiency silicon solar modules such as silicon heterojunction (SHJ) solar modules and tunneling oxide passivated contact (TOPCon) solar modules.

The temperature dependence of full-area aluminum back surface field (Al-BSF) and bifacial passivated emitter and rear cell (PERC) modules has been well investigated. El Achouby et al. [2] and Humada et al. [3] have studied the method to extract physical parameters of diode equivalent circuit modelling a photovoltaic solar module. De Soto et al. [4] have given the variation of current-voltage (I-V) curve with

temperature and irradiance. The variation of parameters for solar modules such as short-circuit current (I_{sc}), open-circuit voltage (V_{oc}), ideality factor etc. with temperature and irradiance have been also conducted [5–11]. In addition, the temperature coefficient of V_{oc} varying with temperature and irradiance has been researched [12–14]. Tian et al. [15] explored the temperature coefficient of fill factor (FF) as a function of irradiance. Skoplaki and Palyvos [16] concerned on the temperature dependence of maximum power (P_m). Wang et al. [17] studied the temperature coefficients for potential-induced degradation (PID) affected solar modules. Green et al. [18], Osterwald et al. [19] and Zhao et al. [20] have presented the test results of the temperature dependence of solar modules. Numerous researchers have investigated the comparison of temperature dependence of various solar modules [21–24]. Based on experimental data, some authors have given some empirical equations and theories [25–29]. In addition to the effects of temperature and irradiance, a number of other influencing factors have also been conducted. Berthod et al. [30] have investigated the effect of relative height of ingot on temperature sensitivity for solar modules.

* Corresponding author.

E-mail address: solargroup@126.com (H. Yang).

Dupre et al. [31] demonstrated the relationship between the temperature dependence of V_{oc} and the external radiative efficiency of solar modules. Hishikawa et al. [32] have given the relationship between temperature coefficients and V_{oc} for solar modules. Some scholars have also calculated the temperature coefficients of solar modules in long term operation [33,34].

As technology matures, TOPCon and SHJ solar modules are gradually commercialized [35–37]. More research is necessary for TOPCon and SHJ solar modules under different module temperature and irradiance. Tuan Le et al. [38] have studied the variation of temperature coefficients for TOPCon solar cells. Le et al. [39] have investigated the temperature-dependent and illumination-dependent of SHJ solar cells. Seif et al. [40], Taguchi et al. [41] and Sachenko et al. [42] studied the relationship between the temperature coefficients of SHJ and temperature. Li et al. [43] studied the influence of irradiance on FF for SHJ. The difference of temperature coefficients between several silicon based solar modules was also investigated [33,44–48].

However, few studies concerned on the temperature coefficients of SHJ and TOPCon solar modules in the same test conditions. In particular, almost no one studied how their temperature dependence changes with temperature and irradiance. In this paper, a series of equations were derived to evaluate temperature dependence of the three modules. The temperature dependence of SHJ and TOPCon solar modules was investigated under a wide range of temperatures and irradiance, PERC solar module was also investigated as a reference. The results indicate that the temperature dependence of I_{sc} is similar for the three modules, and the temperature dependence of I_{sc} is almost invariable with temperature and irradiance. The temperature dependence of V_{oc} and P_m of the three modules decreases with the increase in module temperature and increase with increasing irradiance. The absolute magnitudes of $(\partial P_m / \partial T)/P_m$ for SHJ are about 0.04 %/°C smaller than that of PERC in average, while the absolute magnitudes of $(\partial P_m / \partial T)/P_m$ for TOPCon are about 0.02 %/°C larger than that of PERC in average. It is worth noting that the temperature dependence of FF for SHJ is opposite to that of the other two modules, which is due to the influence of the temperature dependence for series resistance (R_s). In addition, the temperature dependence is obviously not linear at low temperature and irradiance. The conclusions obtained in this article show the specific changes of temperature dependence for the three commercial modules, which provides a reference for the evaluation of the electrical performance of solar modules in the field.

2. Experimental details

In this paper, three types of solar modules are prepared for testing. PERC module has two parallel-connected substrings, each consisting of 75 series-connected 3-cut cells (210 mm × 70 mm). SHJ module has two parallel-connected substrings, each consisting of 60 series-connected half-cut cells (158.75 mm × 79.375 mm). TOPCon module has two parallel-connected substrings, each consisting of 72 series-connected half-cut cells (158.75 mm × 79.375 mm). All the three modules consist of glass superstrate, ethylene-vinyl acetate (EVA), solar cells, EVA, and glass substrate. The typical parameters of the three solar modules are listed in Table 1. Although there are some differences in their specifications, there is no impact on the study of temperature dependence for the three modules.

Table 1
Typical parameters of crystalline silicon solar module under STC.

Parameter	V_{oc} (V)	I_{sc} (A)	V_m (V)	I_m (A)	P_m (W)
PERC	51.01	12.46	42.88	11.68	500
SHJ	44.20	9.82	37.20	9.15	340
TOPCon	50.70	10.29	42.40	9.79	415

STC: 1 kW/m² irradiance, 25 °C module temperature and AM 1.5 global spectrum.

For p-type PERC solar cells, it is passivated by the SiO₂/SiN_x:H ARC stack at the front. On the rear side, the AlO_x/SiN_x:H passivation and rear reflector stack is locally grooved with a laser. Finally, the screen printing and cofiring are used for the front and rear side. For SHJ solar cells, an intrinsic amorphous-Si layer, a doped amorphous-Si layer, and a TCO layer are deposited on both sides of a crystalline-Si substrate. Metal electrodes are formed with the sputtering and screen-printing methods on the both layers. For TOPCon solar cells, there is an n-type c-Si substrate with boron emitter on the front side. The front side is passivated by a dielectric stack of passivation and anti-reflection layer. The rear side features tunnel oxide and doped polysilicon layer acting as passivating carrier-selective contact, stacked with amorphous hydrogenated silicon nitride (a-SiN_x:H) layer as the source of hydrogenation to passivate the dangling bonds in Si-SiO_x interface. Screen-printing of Ag grid is used on the front and rear side.

Several I-V curves of the three modules were measured by solar simulator (XJCM-13A, AAA Class solar simulator, in accordance with IEC 60904-9, 200–1000 W/m²) with thermostatic chamber. The thermostatic chamber was composed of resistance wires, fans and Pt100 temperature sensors. The modules were located in the thermostatic chamber below the light source. I-V curve was traced from I_{sc} to V_{oc} in a single sweep. The thermostatic chamber was heated by resistance wires with a temperature of 25 °C–75 °C. Fans were used to perform forced convection and unify the temperature. Proportional integral derivative controllers were used to control temperature. The temperature of solar module was measured by Pt100, and the measurement method was according to IEC 60891 [49]. The temperature non-uniformity was kept at ±2 °C. The measurement process is shown in Fig. 1. During the measurement process, I-V curves were traced with irradiances from 200 to 1000 W/m² in an interval of 200 W/m². I-V characteristics of the modules were recorded in 5 °C to extract the temperature dependence from 25 °C to 75 °C. In order to ensure the accuracy of the test results, the I-V curves in each condition are measured repeatedly.

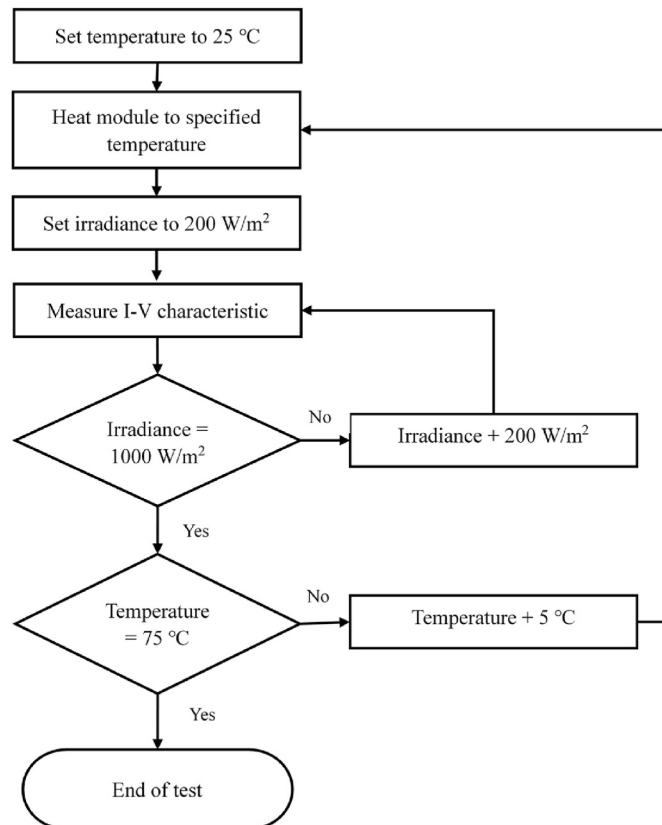


Fig. 1. Measurement process of I-V characteristics test system.

3. Results and discussion

3.1. Theoretical computations of temperature dependence for solar modules

For the single diode model of an ideal solar module, R_s is zero and the shunt resistance (R_{sh}) is infinite. When the solar module is connected to the load, the current passing through the load is:

$$I = I_{ph} - I_0 \left[\exp\left(\frac{qV}{nkT}\right) - 1 \right] \quad (1)$$

Where I is the current flowing through the load, I_{ph} is the photo-generated current, I_0 is the reverse saturation current, q is the elementary charge, V is the voltage across the terminals of load, n is the diode ideality factor, k is the Boltzmann constant, and T is the module temperature in degree Kelvin.

Under the open-circuit condition, $I = 0$ and $V = V_{oc}$, while I_{ph} is equal to the short-circuit current I_{sc} . Isolating V_{oc} , we obtain:

$$V_{oc} = \frac{kT}{q} \ln\left(\frac{I_{sc}}{I_0} + 1\right) \quad (2)$$

Differentiating Eq. (2) with respect to T and dividing by V_{oc} , we obtain:

$$\frac{1}{V_{oc}} \frac{\partial V_{oc}}{\partial T} = \frac{1}{T} + \frac{\frac{1}{I_0} \frac{\partial I_{sc}}{\partial T} - \frac{I_{sc}}{I_0} \frac{\partial I_0}{\partial T}}{\left(\frac{I_{sc}}{I_0} + 1\right) \ln\left(\frac{I_{sc}}{I_0} + 1\right)} \quad (3)$$

For solar cells, $I_{sc} \gg I_0$, so $I_{sc} + I_0 \approx I_{sc}$, which can be substituted into Eq. (3):

$$\frac{1}{V_{oc}} \frac{\partial V_{oc}}{\partial T} = \frac{1}{T} + \left(\frac{1}{I_{sc}} \frac{\partial I_{sc}}{\partial T} - \frac{1}{I_0} \frac{\partial I_0}{\partial T} \right) \frac{1}{\ln I_{sc} - \ln I_0} \quad (4)$$

I_0 is strongly affected by temperature and can be expressed as follow [24]:

$$I_0 = AT^{3+\gamma} \exp\left(-\frac{E_g}{kT}\right) \quad (5)$$

Where E_g is bandgap energy. A is an empirical parameter that doesn't vary with temperature and irradiance. γ is a constant.

After differentiating temperature on both sides of Eq. (5), the expression of $(\partial I_0 / \partial T) / I_0$ can be obtained as follows:

$$\frac{1}{I_0} \frac{\partial I_0}{\partial T} = \frac{3 + \gamma}{T} - \frac{T \frac{\partial E_g}{\partial T} - E_g}{kT^2} \quad (6)$$

E_g can be expressed as follows [26]:

$$E_g = E_g(0) - \frac{\alpha T^2}{\beta + T} \quad (7)$$

$$\frac{\partial E_g}{\partial T} = -\frac{2\alpha\beta T + \alpha T^2}{(\beta + T)^2} \quad (8)$$

Where $E_g(0) = E_g$ at $T = 0$ K, α and β are materials constants.

By substituting both (7) and (8) into (6), we can get the expression of $(\partial I_0 / \partial T) / I_0$:

$$\frac{1}{I_0} \frac{\partial I_0}{\partial T} = \frac{3 + \gamma}{T} + \frac{a\beta}{k(\beta + T)^2} + \frac{E_g(0)}{kT^2} \quad (9)$$

Obviously $(\partial I_0 / \partial T) / I_0$ does not change with irradiance and decreases with increasing temperature.

The temperature dependence of the short circuit current can be written as Eq. (10) [1]:

$$\frac{1}{I_{sc}} \frac{\partial I_{sc}}{\partial T} = \frac{1}{I_{sc,1sun}} \frac{\partial I_{sc,1sun}}{\partial E_g} \frac{\partial E_g}{\partial T} + \frac{1}{f_c} \frac{\partial f_c}{\partial T} \quad (10)$$

Where $I_{sc,1sun}$ is the ideal short circuit current and f_c is the collection fraction. The first right-hand term shows the temperature dependence of the bandgap of materials. The second right-hand term is the temperature dependence of collection fraction.

The equation of $(\partial FF / \partial T) / FF$ can be described by Eq. (11) [20]:

$$\frac{1}{FF} \frac{\partial FF}{\partial T} = (1 - 1.02FF_0) \left(\frac{1}{V_{oc}} \frac{\partial V_{oc}}{\partial T} - \frac{1}{T} \right) - \frac{R_s}{V_{oc}/I_{sc} - R_s} \left(\frac{1}{R_s} \frac{\partial R_s}{\partial T} \right) \quad (11)$$

By bringing Eq. (4) to Eq. (10), we can obtain:

$$\frac{1}{FF} \frac{\partial FF}{\partial T} = (1 - 1.02FF_0) \left[\left(\frac{1}{I_{sc}} \frac{\partial I_{sc}}{\partial T} - \frac{1}{I_0} \frac{\partial I_0}{\partial T} \right) \frac{1}{\ln I_{sc} - \ln I_0} \right] - \frac{R_s}{V_{oc}/I_{sc} - R_s} \left(\frac{1}{R_s} \frac{\partial R_s}{\partial T} \right) \quad (12)$$

The normalized temperature dependence of P_m can be considered as a sum of the normalized temperature dependence of I_{sc} , V_{oc} and FF , which can be represented as:

$$\frac{1}{P_m} \frac{\partial P_m}{\partial T} = \frac{1}{I_{sc}} \frac{\partial I_{sc}}{\partial T} + \frac{1}{V_{oc}} \frac{\partial V_{oc}}{\partial T} + \frac{1}{FF} \frac{\partial FF}{\partial T} \quad (13)$$

It should be pointed out that there exists slight difference between temperature dependence and temperature coefficient of solar module. For a generic variable Z, the temperature dependence of Z is $(\partial Z / \partial T) / Z$, while the temperature coefficient of Z is $(\partial Z / \partial T) / Z_{T_n=25^\circ C}$.

3.2. The temperature dependence for PERC, SHJ and TOPCon as a function of temperature at 1000 W/m²

Fig. 2 shows the measured temperature dependence of three modules as a function of temperature under 1000 W/m². From Fig. 2 (a), it is found that the positive slope of $(\partial I_{sc} / \partial T) / I_{sc}$ upon the temperature shows a constant trend when the temperature increases, which is caused by the narrowing of bandgap energy for pn junction. As shown in Eq. (10), the bandgap and the collection fraction affect the value of $(\partial I_{sc} / \partial T) / I_{sc}$. As the temperature increases, the silicon band gap decreases and more carriers are excited, leading to the increase of I_{sc} . Because the three modules are Si-based solar modules, the values of $(\partial I_{sc} / \partial T) / I_{sc}$ for the three modules are similar at the same temperature. In addition, it is observed that $(\partial I_{sc} / \partial T) / I_{sc}$ of the three modules remain essentially unchanged with temperature, which means that I_{sc} is nearly linear with temperature.

From Fig. 2 (b), with the increase of temperature, the absolute magnitudes of $(\partial V_{oc} / \partial T) / V_{oc}$ for the three modules increase, which means that the influence of temperature on the pn junction recombination rate is increasing. Additionally, it is observed that the absolute magnitude of $(\partial V_{oc} / \partial T) / V_{oc}$ for SHJ is lower than that of PERC and TOPCon. This is because there exists a-Si:H in SHJ. Due to the excellent passivation performance of a-Si:H [36], the absolute magnitude of $(\partial V_{oc} / \partial T) / V_{oc}$ for SHJ is lower than that of PERC and TOPCon. Moreover, it can be observed that at low temperature, the absolute magnitude of $(\partial V_{oc} / \partial T) / V_{oc}$ for TOPCon is slightly lower than that of PERC, but the absolute magnitudes of $(\partial V_{oc} / \partial T) / V_{oc}$ for both modules are nearly the same at high temperature. Therefore, it can be inferred that the passivation performance of TOPCon is slightly better than PERC. Additionally, it is worth noting that the values of $(\partial V_{oc} / \partial T) / V_{oc}$ for the three modules are not linear within the measured temperature, which is most obvious in TOPCon solar module. This should be taken into account when predicting V_{oc} of solar modules in the field.

Fig. 2 (c) shows the temperature dependence of fill factor as a function of temperature. Same as $(\partial V_{oc} / \partial T) / V_{oc}$, the absolute magnitudes of $(\partial FF / \partial T) / FF$ also increase when the temperature increases. The absolute magnitude of $(\partial FF / \partial T) / FF$ for SHJ is the smallest and TOPCon is the largest. Combined with Eq. (10), it can be observed that $(\partial FF / \partial T) / FF$ is related to $(\partial V_{oc} / \partial T) / V_{oc}$ and R_s . Since $(\partial V_{oc} / \partial T) / V_{oc}$ of PERC is similar to TOPCon, R_s becomes the main reason for the difference between them. Obviously TOPCon has a larger R_s than PERC in this

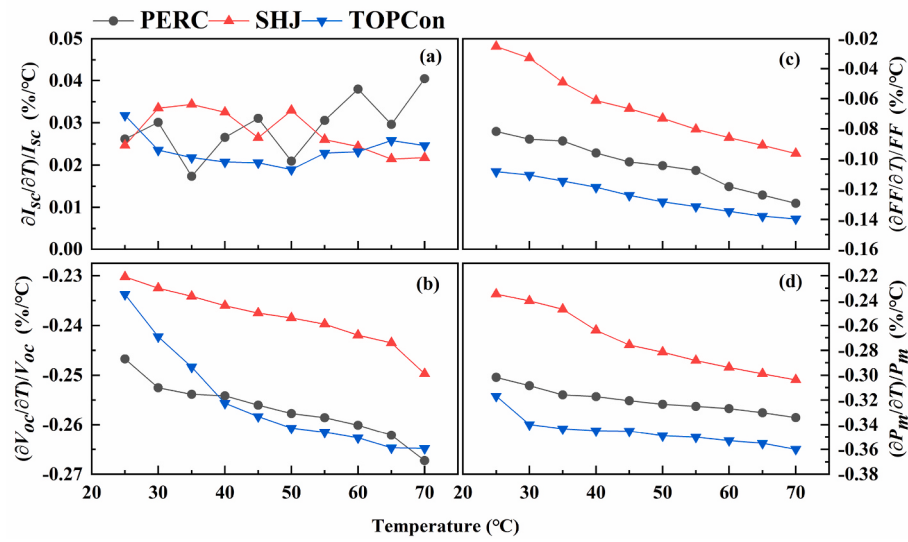


Fig. 2. Measured temperature dependence of (a) I_{sc} , (b) V_{oc} , (c) FF and (d) P_m of three modules as a function of temperature under 1000 W/m^2 .

experiment, which has been confirmed in the subsequent experiments.

Fig. 2 (d) shows the temperature dependence of maximum power as a function of temperature. It is found that the absolute magnitude of $(\partial P_m / \partial T) / P_m$ for SHJ is the smallest, and it is the largest for TOPCon. This is because that the value of $(\partial P_m / \partial T) / P_m$ is the sum of $(\partial I_{sc} / \partial T) / I_{sc}$, $(\partial V_{oc} / \partial T) / V_{oc}$ and $(\partial FF / \partial T) / FF$. Combined with the above analysis of the temperature dependence for the three types of modules, it can be considered that the absolute magnitude of $(\partial P_m / \partial T) / P_m$ for SHJ is the minimum because of the smallest $(\partial V_{oc} / \partial T) / V_{oc}$ and $(\partial FF / \partial T) / FF$. The absolute magnitude of $(\partial P_m / \partial T) / P_m$ for PERC is smaller than that of TOPCon mainly because of the difference in $(\partial FF / \partial T) / FF$. It can be observed that the tendency of $(\partial P_m / \partial T) / P_m$ versus temperature for PERC and TOPCon is almost the same, which is because the cell structures of them are similar. It can be also observed that the values of $(\partial P_m / \partial T) / P_m$ for the three modules are not linear over the full temperature range, which increases the difficulty of power prediction of solar modules at different operating temperature.

Through the analysis of $(\partial FF / \partial T) / FF$, the importance of R_s to FF has already been mentioned. Therefore, according to the determination method of R_s in IEC 60891 [49], the series resistance of the three modules versus temperature under 1000 W/m^2 is calculated and shown in Fig. 3. As predicted above, R_s of TOPCon is larger than that of PERC. With the increase of temperature, lattice scattering of doped silicon increases, which leads to the increase of R_s for PERC and TOPCon. However, due to the influence of intrinsic amorphous-Si layer on R_s [41], R_s of SHJ decreases with increasing temperature, which is used in Section 3.3. In addition, the variation tendencies of R_s for PERC and TOPCon are almost the same with the increasing temperature, which results from the similar cell structure of the two modules.

3.3. The temperature dependence for PERC, SHJ and TOPCon as a function of irradiance

Fig. 4 shows the measured temperature dependence of short-circuit current as a function of irradiance. From Fig. 4, it is observed that there exists some fluctuation about the value of $(\partial I_{sc} / \partial T) / I_{sc}$, which could be caused by measurement uncertainty of $(\partial I_{sc} / \partial T) / I_{sc}$. Combined Fig. 4 with the associated uncertainty, we consider that the values of $(\partial I_{sc} / \partial T) / I_{sc}$ for the three modules do not change with irradiance. This conclusion is consistent with Eq. (10). In Eq. (10), the value of $(\partial I_{sc} / \partial T) / I_{sc}$ varies with bandgap and collection fraction, which does not vary with irradiance. Moreover, in Section 3.2, we find that $(\partial I_{sc} / \partial T) / I_{sc}$ of the three modules remain essentially unchanged with temperature.

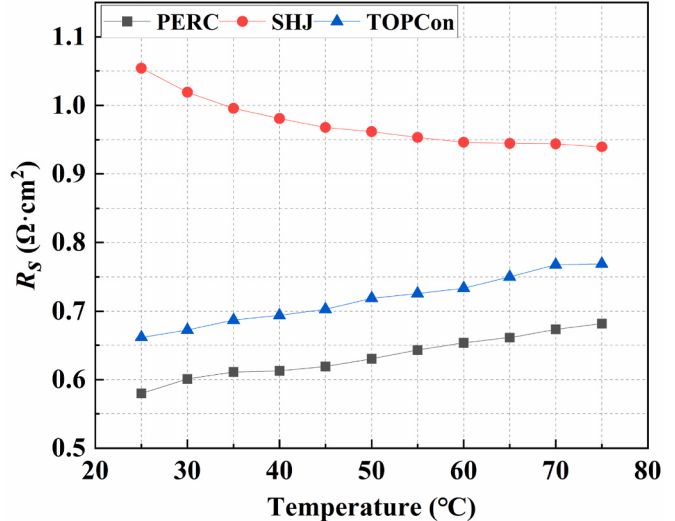


Fig. 3. Measured R_s as a function of temperature at 1000 W/m^2 .

Therefore, it can be considered that the values of $(\partial I_{sc} / \partial T) / I_{sc}$ for the three modules are fixed in the field.

Fig. 5 depicts the measured temperature dependence of open-circuit voltage as a function of irradiance. As shown in Fig. 5, it is found that with the increase of irradiance, the absolute magnitudes of $(\partial V_{oc} / \partial T) / V_{oc}$ gradually decrease. When irradiance varies from 200 W/m^2 to 1000 W/m^2 , the value of $(\partial V_{oc} / \partial T) / V_{oc}$ for PERC varies from $-0.27 \%/\text{°C}$ to $-0.245 \%/\text{°C}$ under 25°C module temperature. The value of $(\partial V_{oc} / \partial T) / V_{oc}$ for SHJ increases from $-0.25 \%/\text{°C}$ to $-0.23 \%/\text{°C}$ as irradiance increase from 200 W/m^2 to 1000 W/m^2 at 25°C . The increasing percent for value of $(\partial V_{oc} / \partial T) / V_{oc}$ varies from $-0.28 \%/\text{°C}$ at 200 W/m^2 to $-0.24 \%/\text{°C}$ at 1000 W/m^2 under 25°C for TOPCon. The results indicate that the absolute magnitude of $(\partial V_{oc} / \partial T) / V_{oc}$ for SHJ is the smallest, and the values of $(\partial V_{oc} / \partial T) / V_{oc}$ for PERC and TOPCon are approximate at any irradiance, which means that the passivation performance of SHJ is the best. Another finding is that the relationship between $(\partial V_{oc} / \partial T) / V_{oc}$ and irradiance is not linear, which can be explained by Eq. (4). According to Eq. (4), since I_{sc} increases linearly with irradiance, and $(\partial I_0 / \partial T) / I_0$ does not change with irradiance, the value of $(\partial V_{oc} / \partial T) / V_{oc}$ for the three modules should be positively correlated with $-1/\ln G$. The difference in I_0 leads to the difference in

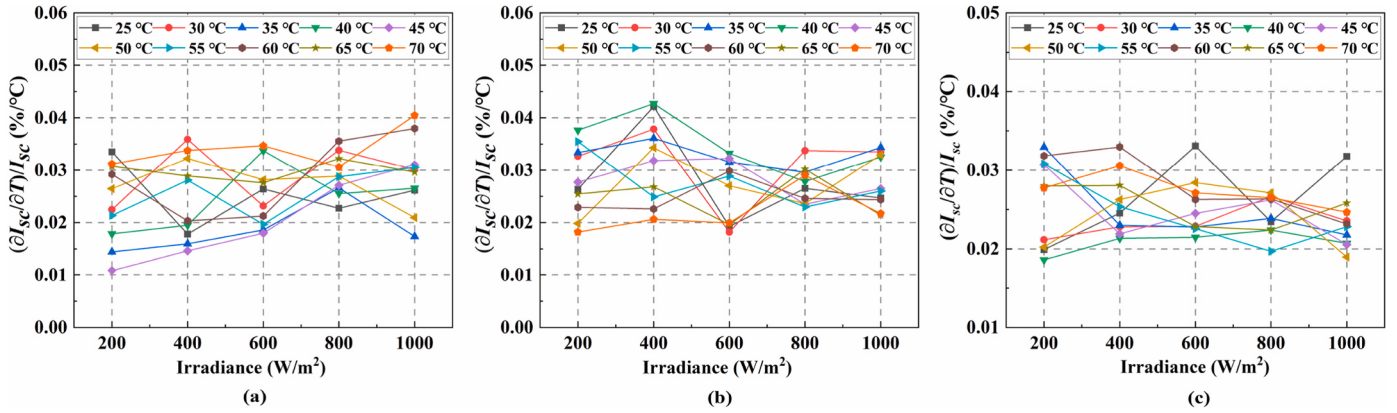


Fig. 4. Measured temperature dependence of short-circuit current as a function of irradiance for (a) PERC, (b) SHJ and (c) TOPCon solar modules.

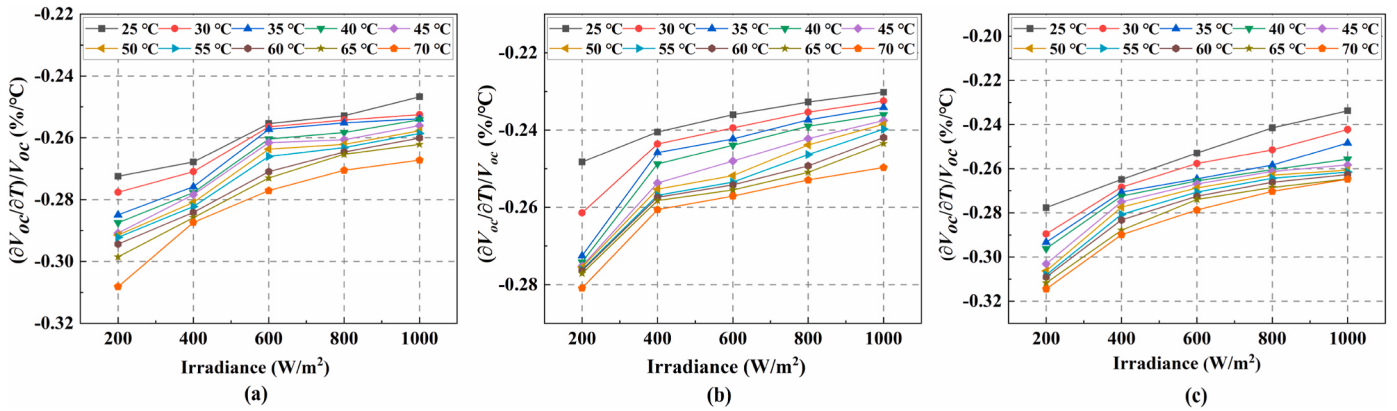


Fig. 5. Measured temperature dependence of open-circuit voltage as a function of irradiance for (a) PERC, (b) SHJ and (c) TOPCon solar modules.

the absolute magnitudes of $(\partial V_{oc} / \partial T) / V_{oc}$ for the three modules. The inferred results are consistent with the experimental results in Fig. 5.

Fig. 6 displays the measured temperature dependence of fill factor versus irradiance. As seen in Fig. 6, the value of $(\partial FF / \partial T) / FF$ for PERC decreases from $-0.06 \%/\text{°C}$ at 200 W/m^2 to $-0.08 \%/\text{°C}$ at 1000 W/m^2 under 25°C module temperature. The value of $(\partial FF / \partial T) / FF$ for SHJ increases from $-0.08 \%/\text{°C}$ to $-0.02 \%/\text{°C}$ as irradiance increase from 200 W/m^2 to 1000 W/m^2 at 25°C . The value of $(\partial FF / \partial T) / FF$ for TOPCon varies from $-0.09 \%/\text{°C}$ at 200 W/m^2 to $-0.11 \%/\text{°C}$ at 1000 W/m^2 under 25°C module temperature. In addition, it can be observed that the value of $(\partial FF / \partial T) / FF$ for SHJ increases with the increase of irradiance, which is opposite to PERC and TOPCon modules. In order to

explore this phenomenon, we discussed $(\partial FF / \partial T) / FF$ from Eq. (12).

The first term of Eq. (12) describes the effect of $(\partial V_{oc} / \partial T) / V_{oc}$ on $(\partial FF / \partial T) / FF$. It is clear that the trend of the first term in Eq. (12) for three modules is consistent. The effect of $(\partial R_s / \partial T) / R_s$ on $(\partial FF / \partial T) / FF$ is shown in the second term of Eq. (12). As irradiance increases, $\frac{1}{(V_{oc}/I_{sc}) - R_s}$ increases. Therefore, with the increase of irradiance, the second term in Eq. (12) becomes the main factor affecting the value of $(\partial FF / \partial T) / FF$. The value of $(\partial R_s / \partial T) / R_s$ for PERC and TOPCon is positive, which results in a negative correlation between $(\partial FF / \partial T) / FF$ and irradiance for these two modules. The value of $(\partial FF / \partial T) / FF$ for SHJ increases with the increase of irradiance due to the negative temperature dependence of R_s . It can also be observed that the variation of $(\partial FF / \partial T) / FF$ for SHJ is not

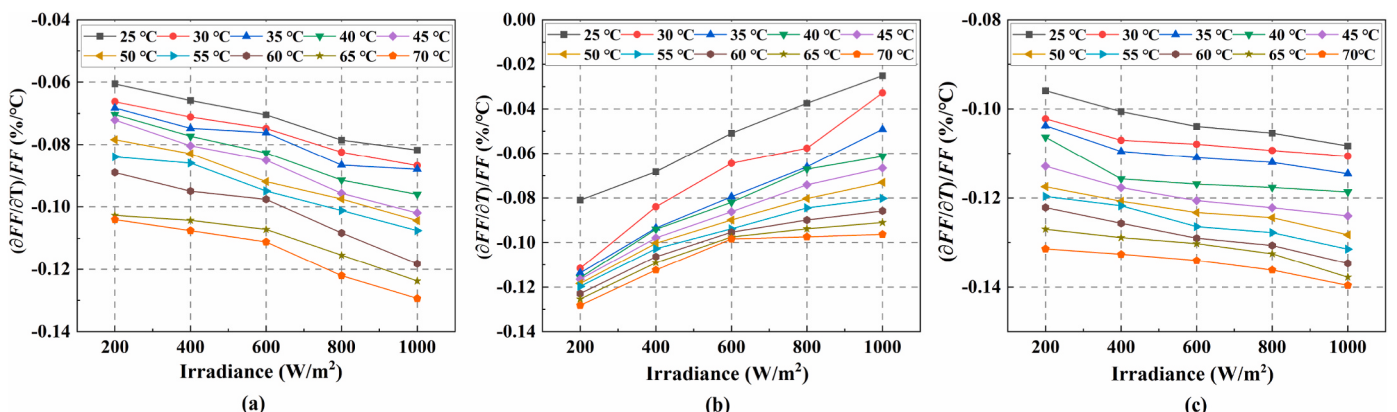


Fig. 6. Measured temperature dependence of fill factor as a function of irradiance for (a) PERC, (b) SHJ and (c) TOPCon solar modules.

uniform under different temperature, which means that the influencing factors of $(\partial FF / \partial T) / FF$ for SHJ under low light conditions are more complex and need to be further studied.

Fig. 7 shows the measured temperature dependence of maximum power as a function of irradiance. From Fig. 7, it can be observed that with the increase of irradiance, the value of $(\partial P_m / \partial T) / P_m$ for PERC increases from $-0.33\%/\text{°C}$ to $-0.30\%/\text{°C}$ under 25 °C . The value of $(\partial P_m / \partial T) / P_m$ for SHJ increases from $-0.30\%/\text{°C}$ at 200 W/m^2 to $-0.24\%/\text{°C}$ at 1000 W/m^2 under 25 °C . The value of $(\partial P_m / \partial T) / P_m$ for TOPCon increases from $-0.35\%/\text{°C}$ at 200 W/m^2 to $-0.32\%/\text{°C}$ at 1000 W/m^2 . It can be found that the absolute magnitude of $(\partial P_m / \partial T) / P_m$ decreases as irradiance increases under the same module temperature. Moreover, it can also be observed that the absolute magnitude of $(\partial P_m / \partial T) / P_m$ for SHJ is the smallest, which is more obvious at high irradiance. The absolute magnitude of $(\partial P_m / \partial T) / P_m$ for TOPCon is larger than that of PERC, which is mainly due to the difference in $(\partial FF / \partial T) / FF$ for PERC and TOPCon solar module. Combining Figs. 4, Figs. 5 and 6, it is found that although $(\partial P_m / \partial T) / P_m$ is mainly influenced by $(\partial V_{oc} / \partial T) / V_{oc}$, the influence of $(\partial FF / \partial T) / FF$ is also another important factor.

3.4. Percentage contribution of the temperature dependence to $(\partial P_m / \partial T) / P_m$ for PERC, SHJ and TOPCon solar modules

Fig. 8 displays percentage contribution of the temperature dependence to $(\partial P_m / \partial T) / P_m$ of three types of solar modules. From Fig. 8, it is obvious that the contribution of $(\partial I_{sc} / \partial T) / I_{sc}$ to $(\partial P_m / \partial T) / P_m$ is the smallest, which means the impact of $(\partial I_{sc} / \partial T) / I_{sc}$ on $(\partial P_m / \partial T) / P_m$ is weak. The value of $(\partial V_{oc} / \partial T) / V_{oc}$ contributes the most to $(\partial P_m / \partial T) / P_m$, so the smaller the absolute magnitude of $(\partial V_{oc} / \partial T) / V_{oc}$, the smaller the absolute magnitude of $(\partial P_m / \partial T) / P_m$. The contribution of $(\partial FF / \partial T) / FF$ fluctuates greatly. With the increase of irradiance, the contribution of $(\partial FF / \partial T) / FF$ to $(\partial P_m / \partial T) / P_m$ for PERC and TOPCon increases while for SHJ decreases. This is consistent with the trend shown in Figs. 5 and 6.

With the increase of temperature, the percentage contribution of $(\partial FF / \partial T) / FF$ for the three modules increases. This indicates that the influence of temperature on $(\partial FF / \partial T) / FF$ is greater than that of $(\partial V_{oc} / \partial T) / V_{oc}$. Therefore, $(\partial FF / \partial T) / FF$ should be focused on when studying the influence of temperature on the temperature dependence of solar modules.

4. Conclusions

In this contribution, the temperature dependence of SHJ and TOPCon solar modules was studied based on theoretical analysis and extensive experimental measurements, and PERC solar modules were considered as a reference. The results show that there is no significant difference in $(\partial I_{sc} / \partial T) / I_{sc}$ for PERC, SHJ and TOPCon solar modules. In addition, the values of $(\partial I_{sc} / \partial T) / I_{sc}$ for the three modules are constant in

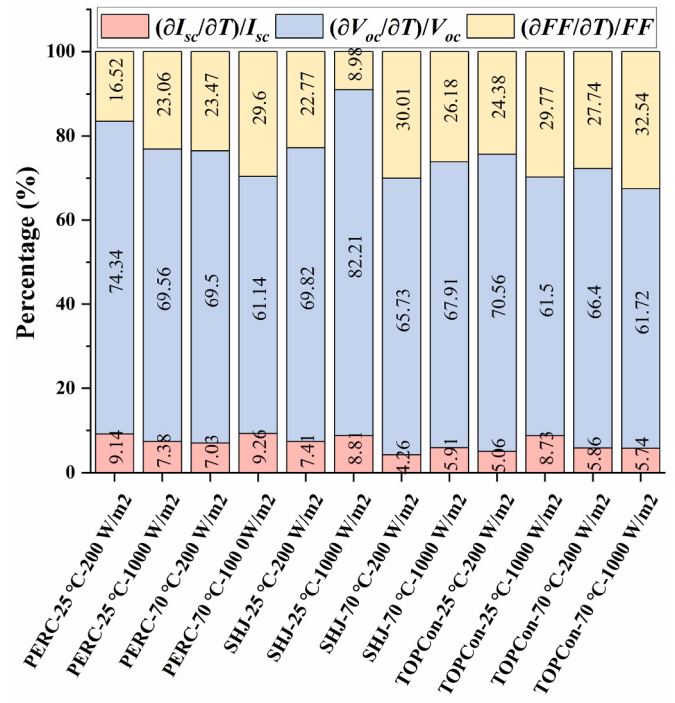


Fig. 8. Percentage contribution of $(\partial I_{sc} / \partial T) / I_{sc}$, $(\partial V_{oc} / \partial T) / V_{oc}$ and $(\partial FF / \partial T) / FF$ to $(\partial P_m / \partial T) / P_m$ of three types of solar modules.

the field. The absolute magnitudes of $(\partial V_{oc} / \partial T) / V_{oc}$ increase with the increasing temperature and the decreasing irradiance. It is clear that the absolute magnitudes of $(\partial V_{oc} / \partial T) / V_{oc}$ for SHJ are the smallest with irradiance from 200 to 1000 W/m^2 and temperature from 25 to 75 °C , and the absolute magnitudes of $(\partial V_{oc} / \partial T) / V_{oc}$ for PERC and TOPCon are similar. This is because that the passivation performance of SHJ is better than that of PERC and TOPCon. An interesting found is that the value of $(\partial FF / \partial T) / FF$ for SHJ increases with the increase of irradiance, which is opposite to PERC and TOPCon modules. This is because as irradiance increases, the effect of R_s on $(\partial FF / \partial T) / FF$ increases. Since R_s of SHJ is a negative temperature dependence, the value of $(\partial FF / \partial T) / FF$ increases with the increase of irradiance. The values of $(\partial R_s / \partial T) / R_s$ for PERC and TOPCon solar modules are positive, which leads to the opposite trend between the two modules and SHJ solar module. The tendency of $(\partial P_m / \partial T) / P_m$ is the same as that of $(\partial V_{oc} / \partial T) / V_{oc}$. However, due to the effect of $(\partial FF / \partial T) / FF$, the absolute magnitudes of $(\partial P_m / \partial T) / P_m$ for SHJ are about $0.04\%/\text{°C}$ smaller than that of PERC, while the absolute magnitudes of $(\partial P_m / \partial T) / P_m$ for TOPCon are about $0.02\%/\text{°C}$ larger than that of PERC. It can also be noted that the value of $(\partial P_m / \partial T) / P_m$

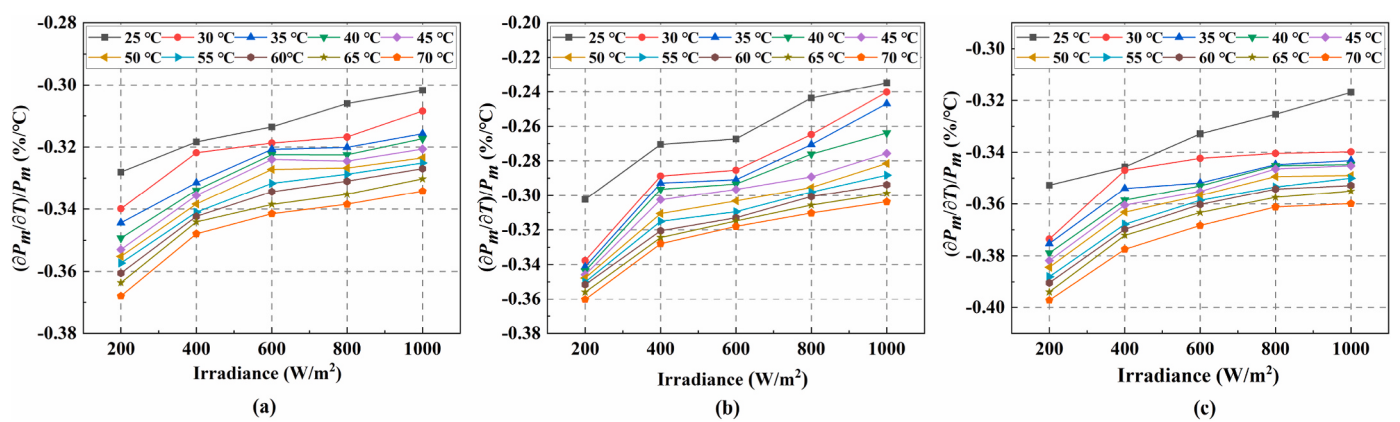


Fig. 7. Measured temperature dependence of maximum power as a function of irradiance for (a) PERC, (b) SHJ and (c) TOPCon solar modules.

presents a nonlinear trend at low temperature and irradiance. The conclusions obtained in this article can provide a reference for the evaluation of the electrical performance of solar modules in the field.

CRediT authorship contribution statement

Chenhui Nan: Writing – review & editing, Writing – original draft, Investigation, Formal analysis, Conceptualization. **Yuanpang Hao:** Writing – review & editing. **Xin Huang:** Writing – review & editing. **He Wang:** Methodology. **Hong Yang:** Writing – review & editing, Methodology, Funding acquisition, Conceptualization.

Declaration of competing interest

The authors declare that they have no known competing financial interests or personal relationships that could have appeared to influence the work reported in this paper.

Data availability

Data will be made available on request.

Acknowledgements

The authors would like to thank the support of the Key Research and Development Projects of Shaanxi Province (Grant No. 2023KXJ-210).

References

- [1] M.A. Green, General temperature dependence of solar cell performance and implications for device modelling, *Prog. Photovoltaics Res. Appl.* 11 (2003) 333–340.
- [2] H. El Achouby, M. Zaimi, A. Ibral, E.M. Assaid, New analytical approach for modelling effects of temperature and irradiance on physical parameters of photovoltaic solar module, *Energy Convers. Manag.* 177 (2018) 258–271.
- [3] A.M. Humada, M. Hojabri, S. Mekhilef, H.M. Hamada, Solar cell parameters extraction based on single and double-diode models: a review, *Renewable Sustainable Energy Rev.* 56 (2016) 494–509.
- [4] W. De Soto, S.A. Klein, W.A. Beckman, Improvement and validation of a model for photovoltaic array performance, *Sol. Energy* 80 (2006) 78–88.
- [5] Q. Bai, C. Nan, L. Zhou, Y. Yang, S. Mao, H. Han, H. Yang, H. Wang, Effect of temperature on ideality factor for PERC monofacial crystalline silicon solar module, in: 2021 IEEE 48th Photovoltaic Specialists Conference (PVSC), 2021, pp. 244–247.
- [6] Q. Bai, H. Tian, C. Nan, L. Ouyang, Y. Zhang, J. Ma, S. Mao, H. Han, H. Yang, H. Wang, Investigation on bifaciality factor and ideality factor of PERC bifacial solar module under different irradiances, in: 2021 IEEE 48th Photovoltaic Specialists Conference (PVSC), 2021, pp. 248–251.
- [7] D.T. Cottas, P.A. Cottas, O.M. Machidon, Study of temperature coefficients for parameters of photovoltaic cells, *Int. J. Photoenergy* (2018) 1–12, 2018.
- [8] E. Cuce, P.M. Cuce, T. Bali, An experimental analysis of illumination intensity and temperature dependency of photovoltaic cell parameters, *Appl. Energy* 111 (2013) 374–382.
- [9] B. Hüttl, L. Gottschalk, S. Schneider, D. Pflaum, A. Schulze, Accurate performance rating of photovoltaic modules under outdoor test conditions, *Sol. Energy* 177 (2019) 737–745.
- [10] C.S. Ruschel, F.P. Gasparin, A. Krenzinger, Experimental analysis of the single diode model parameters dependence on irradiance and temperature, *Sol. Energy* 217 (2021) 134–144.
- [11] P. Singh, S. Singh, M. Lal, M. Husain, Temperature dependence of I–V characteristics and performance parameters of silicon solar cell, *Sol. Energy Mater. Sol. Cells* 92 (2008) 1611–1616.
- [12] W. Bagienski, G.S. Kinsey, M. Liu, A. Nayak, V. Garboushian, Open circuit voltage temperature coefficients vs. concentration: theory, indoor measurements, and outdoor measurements, *AIP Conf. Proc.* 1477 (2012) 148–151.
- [13] R. Dubey, P. Batra, S. Chattopadhyay, A. Kottantharayil, B.M. Arora, K. L. Narasimhan, J. Vasi, Measurement of temperature coefficient of photovoltaic modules in field and comparison with laboratory measurements, in: 2015 IEEE 42th Photovoltaic Specialists Conference (PVSC), IEEE, 2015, pp. 1–5.
- [14] T. Tiedje, D.A. Engelbrecht, Temperature dependence of the limiting efficiency of bifacial silicon solar cells, in: 2020 IEEE 47th Photovoltaic Specialists Conference (PVSC), 2020, pp. 1789–1791.
- [15] H. Tian, Q. Bai, X. Li, H. Han, S. Maoa, H. Yang, H. Wang, Comparative study on fill factor of PERC Silicon Solar cells and Al-BSF Silicon solar cells under non-standard test conditions, in: 2021 IEEE 48th Photovoltaic Specialists Conference (PVSC), 2021, pp. 256–259.
- [16] E. Skoplaki, J.A. Palyvos, On the temperature dependence of photovoltaic module electrical performance: a review of efficiency/power correlations, *Sol. Energy* 83 (2009) 614–624.
- [17] H. Wang, X. Cheng, H. Yang, W. He, Z. Chen, L. Xu, D. Song, Potential-induced degradation: recombination behavior, temperature coefficients and mismatch losses in crystalline silicon photovoltaic power plant, *Sol. Energy* 188 (2019) 258–264.
- [18] M.A. Green, K. Emery, A.W. Blakers, Silicon solar cells with reduced temperature sensitivity, *Electron. Lett.* 18 (1982).
- [19] C.R. Osterwald, T. Glatfelter, J. Burdick, Comparison of the temperature coefficients of the basic I–V parameters for various types of solar cells, in: Conference Record of the IEEE Photovoltaic Specialists Conference, 1987, pp. 188–193, 193.
- [20] J. Zhao, A. Wang, S.J. Robinson, M.A. Green, Reduced temperature coefficients for recent high-performance silicon solar cells, *Prog. Photovoltaics Res. Appl.* 2 (1994) 221–225, 225.
- [21] C. Berthod, R. Strandberg, G.H. Yordanov, H.G. Beyer, J.O. Odden, On the variability of the temperature coefficients of mc-Si solar cells with irradiance, *Energy Proc.* 92 (2016) 2–9.
- [22] K. Emery, J. Burdick, Y. Caiyem, D. Dunlavay, H. Field, B. Kroposki, T. Moriarty, L. Ottoson, S. Rummel, T. Strand, M.W. Wanlass, Temperature dependence of photovoltaic cells, modules and systems, in: Conference Record of the Twenty Fifth IEEE Photovoltaic Specialists Conference, 1996, pp. 1275–1278.
- [23] F. Perin Gasparin, F. Detzel Kipper, F. Schuck de Oliveira, A. Krenzinger, Assessment on the variation of temperature coefficients of photovoltaic modules with solar irradiance, *Sol. Energy* 244 (2022) 126–133.
- [24] H. Wang, X. Cheng, H. Yang, Temperature coefficients and operating temperature verification for passivated emitter and rear cell bifacial silicon solar module, *IEEE J. Photovoltaics* 10 (2020) 729–739.
- [25] O. Dupré, R. Vaillon, M.A. Green, Physics of the temperature coefficients of solar cells, *Sol. Energy Mater. Sol. Cells* 140 (2015) 92–100.
- [26] J.C.C. Fan, Theoretical temperature dependence of solar cell parameters, *Sol. Cell.* 17 (1986) 309–315, 315.
- [27] G.M.N. Javier, P. Dwivedi, Y. Buratti, I. Perez-Wurfl, T. Trupke, Z. Hameiri, Improvements and gaps in the empirical expressions for the fill factor of modern industrial solar cells, *Sol. Energy Mater. Sol. Cells* (2023) 253.
- [28] P. Singh, N.M. Ravindra, Temperature dependence of solar cell performance—an analysis, *Sol. Energy Mater. Sol. Cells* 101 (2012) 36–45.
- [29] H. Steinkemper, I. Geisemeyer, M.C. Schubert, W. Warta, S.W. Glunz, Temperature-dependent modeling of silicon solar cells—eg, n i, recombination, and VOC, *IEEE J. Photovoltaics* 7 (2017) 450–457.
- [30] C. Berthod, R. Strandberg, J.O. Odden, T.O. Saetre, Reduced temperature sensitivity of multicrystalline silicon solar cells with low ingot resistivity, in: 2016 IEEE 43th Photovoltaic Specialists Conference (PVSC), 2016, pp. 2398–2402.
- [31] O. Dupre, R. Vaillon, M.A. Green, Experimental assessment of temperature coefficient theories for silicon solar cells, *IEEE J. Photovoltaics* 6 (2016) 56–60.
- [32] Y. Hisikawa, T. Doi, M. Higa, K. Yamagoe, H. Ohshima, T. Takenouchi, M. Yoshita, Voltage-dependent temperature coefficient of the I–V curves of crystalline silicon photovoltaic modules, *IEEE J. Photovoltaics* 8 (2018) 48–53.
- [33] B.R. Paudyal, A.G. Imenes, Investigation of temperature coefficients of PV modules through field measured data, *Sol. Energy* 224 (2021) 425–439.
- [34] M. Piliougine, A. Oukaja, M. Sidrach-de-Cardona, G. Spagnuolo, Temperature coefficients of degraded crystalline silicon photovoltaic modules at outdoor conditions, *Prog. Photovoltaics Res. Appl.* 29 (2021) 558–570.
- [35] T. Mishima, M. Taguchi, H. Sakata, E. Maruyama, Development status of high-efficiency HIT solar cells, *Sol. Energy Mater. Sol. Cells* 95 (2011) 18–21.
- [36] M. Taguchi, A. Terakawa, E. Maruyama, M. Tanaka, Obtaining a higher Voc in HIT cells, *Prog. Photovoltaics Res. Appl.* 13 (2005) 481–488.
- [37] H. Wei, Y. Zeng, J. Zheng, Z. Yang, M. Liao, S. Huang, B. Yan, J. Ye, Unraveling the passivation mechanisms of c-Si/SiO_x/poly-Si contacts, *Sol. Energy Mater. Sol. Cells* (2023) 250.
- [38] A.H. Tuan Le, R. Basnet, D. Yan, W. Chen, N. Nandakumar, S. Duttagupta, J.P. Seif, Z. Hameiri, Temperature-dependent performance of silicon solar cells with polysilicon passivating contacts, *Sol. Energy Mater. Sol. Cells* (2021) 225.
- [39] A.H.T. Le, A. Srinivasa, S.G. Bowden, Z. Hameiri, A. Augusto, Temperature and illumination dependence of silicon heterojunction solar cells with a wide range of wafer resistivities, *Prog. Photovoltaics Res. Appl.* 31 (2022) 536–545.
- [40] J.P. Seif, G. Krishnamani, B. Demaurex, C. Ballif, S.D. Wolf, Amorphous/crystalline silicon interface passivation: ambient-temperature dependence and implications for solar cell performance, *IEEE J. Photovoltaics* 5 (2015) 718–724.
- [41] M. Taguchi, E. Maruyama, M. Tanaka, Temperature dependence of amorphous/crystalline silicon heterojunction solar cells, *Jpn. J. Appl. Phys.* 47 (2008) 814–818.
- [42] A.V. Sachenko, Y.V. Kryuchenko, V.P. Kostylyov, A.V. Bobyl, E.I. Terukov, S. N. Abolmasov, A.S. Abramov, D.A. Andronikov, M.Z. Shvarts, I.O. Sokolovskyi, M. Evstigneev, Temperature dependence of photoconversion efficiency in silicon heterojunction solar cells: theory vs experiment, *J. Appl. Phys.* 119 (2016).
- [43] X. Li, Y. Yang, S. Huang, K. Jiang, Z. Li, W. Zhao, J. Yu, Q. Gao, A. Han, J. Shi, J. Du, F. Meng, L. Zhang, Z. Liu, W. Liu, Reassessment of silicon heterojunction cell performance under operating conditions, *Sol. Energy Mater. Sol. Cells* (2022) 247.
- [44] J. Haschke, J.P. Seif, Y. Riesen, A. Tomasi, J. Cattin, L. Tous, P. Choulat, M. Aleman, E. Cornagliotti, A. Urueña, R. Russell, F. Duerinckx, J. Champliaud, J. Levrat, A.A. Abdallah, B. Aissa, N. Tabet, N. Wyrsch, M. Despeisse, J. Szlufcik, S. De Wolf, C. Ballif, The impact of silicon solar cell architecture and cell interconnection on energy yield in hot & sunny climates, *Energy Environ. Sci.* 10 (2017) 1196–1206.

- [45] P. Kamkird, N. Ketjoy, W. Rakwichian, S. Sukchai, Investigation on temperature coefficients of three types photovoltaic module technologies under Thailand operating condition, *Procedia Eng.* 32 (2012) 376–383.
- [46] M. Kasu, J. Abdu, S. Hara, S. Choi, Y. Chiba, A. Masuda, Temperature dependence measurements and performance analyses of high-efficiency interdigitated back-contact, passivated emitter and rear cell, and silicon heterojunction photovoltaic modules, *Jpn. J. Appl. Phys.* 57 (2018).
- [47] J. Lopez-Garcia, D. Pavanello, T. Sample, Analysis of temperature coefficients of bifacial crystalline silicon PV modules, *IEEE J. Photovoltaics* 8 (2018) 960–968.
- [48] S.M.F. Zhang, J.P. Seif, M.D. Abbott, A.H.T. Le, T.G. Allen, I. Perez-Wurfl, Z. Hameiri, Illumination-dependent temperature coefficients of the electrical parameters of modern silicon solar cell architectures, *Nano Energy* 98 (2022).
- [49] IEC 60891, International Standard IEC 60891 - Photovoltaic Devices - Procedures for Temperature and Irradiance Corrections to Measured I-V Characteristics, 2.0, International Electrotechnical Commission (IEC), Geneva, 2009.